ELSEVIER

Chemical Engineering Journal 130 (2007) 111–118

Chemical Engineering Journal

www.elsevier.com/locate/cej

Tomographic imaging of counter-current bubbly flow by wire mesh tomography

N. Fuangworawong [a,*], H. Kikura [b,1], M. Aritomi [b,1], T. Komeno [c]

[a] *Department of Mechanical Engineering, Faculty of Engineering, Chulalongkorn University, Wang Mai, Pathum Wan, Bangkok 10330, Thailand*
[b] *Research Laboratory for Nuclear Reactor, Tokyo Institute of Technology, 2-12-1, Ohokayama, Meguro-ku, 152-8550 Tokyo, Japan*
[c] *The Japan Atomic Power Company, 1-1, Kandamitoshiro-cho, Chiyoda-ku, 101-0053 Tokyo, Japan*

Abstract

The objective of this work is to investigate characteristics of counter-current bubbly flow in a circular pipe with an inner diameter of 50 mm by using wire mesh tomography (WMT). The accuracy of WMT on void fraction measurement is also clarified by comparing the result with a non-intrusive optical method. The accuracy is within ±10%. Local void fractions of many flow conditions are reported. Local void fraction profile affected by superficial liquid velocity and bubble size is shown and discussed. Furthermore, intrusive effects, including bubble break-up and bubble deceleration, are also investigated. Bubbles passing a transparent wire mesh sensor (WMS) are investigated by the optical method. It is shown that bubbles are broken and decelerated by wires of the sensor. It can be concluded that the bubble break-up rate increase with increasing of bubble velocity. However, the bubble deceleration is not depending on the bubble velocity.

Keywords: Wire mesh tomography; Counter-current flow; Intrusive effect; Void fraction

1. Introduction

Counter-current bubbly flow plays an important role for many industries, in particular, chemical industry. Both mathematical model and measurement method have been researched and developed for many decades to clarify two-phase characteristics. Void fraction is an important parameter out of many parameters in a study of two-phase flow dynamics. Characteristics of void fraction have been investigated by many researchers. Yamaguchi and Yasaburo [1] investigated cross-sectional void fractions of co-current and counter-current air–water flow in vertical pipes with an inner diameter of 40 and 80 mm. The cross-sectional void fraction was measured by a quick-closing valve method. The experiments were carried out in bubbly and slug flow regimes. A correlation for predicting the void fraction of the counter-current air–water flow in the vertical pipe was proposed. Hasan et al. [2] also investigated cross-sectional void fractions of co-current and counter-current flow in a vertical pipe with an inner diameter of 127 mm. The flow system is an air–water system. The cross-sectional void fraction was calculated from a pressure drop measured across two points. This experiment was also carried out in bubbly and slug flow regimes. A model for estimating the void fraction of the counter-current flow based on the drift-flux approach in the big diameter pipe was proposed. However, local void fraction in the counter-current bubbly flow was not investigated and reported in these work because of a limitation of the measuring methods. Aritomi et al. [3–5] investigated the behaviours of counter-current bubbly flow in a rectangular channel. Local void fraction was measured by a non-optical method. The accuracy of cross-sectional void fraction was clarified by comparing the result with the one calculated from a differential pressure method. Characteristics of the local void fraction depending on the liquid and gas velocity were investigated. However, the optical method is labor-intensive and can only be used in low void fraction condition.

Two-phase flow measuring methods can be divided into two groups including of a non-intrusive and an intrusive method. The advantage of the intrusive method is a capability of local parameters measurement. However, one of the important disadvantages is intrusive effect on the two-phase flow. Wire mesh tomography (WMT) method is one of many intrusive methods. WMT can obtain local void fraction by measuring electrical conductivity between pairs of crossing wires. There are several studies using WMT to investigate characteristics of bubbly flow [6–8]. Furthermore, the accuracy of WMT was also clarified by comparing with other non-intrusive methods, optical and X-

* Corresponding author. Tel.: +81 3 5734 3063; fax: +81 3 5734 2959.
E-mail address: nattadate@2phase.nr.titech.ac.jp (N. Fuangworawong).
[1] Tel.: +81 3 5734 3063; fax: +81 3 5734 2959.

1385-8947/$ – see front matter © 2006 Elsevier B.V. All rights reserved.
doi:10.1016/j.cej.2006.08.033

Nomenclature

J_G	superficial gas velocity (mm/s)
J_L	superficial liquid velocity (mm/s)
t	time (s)
V	voltage
x	position (mm)
y	position (mm)
Greek letter	
ε	local void fraction

ray methods [9,10]. However, all of the work was studied in a co-current and stagnant flow.

From this view point, the objective of this work is to clarify the accuracy of the void fraction measurement by comparing the result with a non-intrusive optical method and to investigate the local void fraction of counter-current bubbly flow. Furthermore, the intrusive effects by wire mesh sensor (WMS), including bubble break-up and bubble deceleration, in the counter-current bubbly flow are also investigated.

2. Experimental setup

The experimental apparatus used in this work is a vertical acrylic pipe with an inside diameter of 50 mm as illustrated in Fig. 1. The total height of the apparatus is about 7 m. This apparatus is an air–water system controlled temperature at 20 ± 2 °C. Flow rate of air and laminar flow meters, including of Sokken Co. Ltd. Model LEF-5LMS for low gas flow rate and Model LFE-300CCM for high gas flow rate (no. 16) and an orifice flow meter (no. 6), respectively. Water is supplied from a lower tank (no. 7) to an upper tank (no. 2) by a pump (no. 1). Water flows downward into a test section pipe by gravity. Water flow rate is controlled by using control valves (no. 8). Air is injected through the bubble generator (no. 4) as illustrated in Fig. 2. Bubbles are generated by composing of liquid flow and air flow. Air is supplied from an air chamber through holes with an inner diameter of 0.2 mm and injected into a pipe through an annular of 1 mm [11]. Flow conditions of this work are at the values of $J_G = 2$, 6, 8, 10 and 20 mm/s, corresponding to voltages of 1.66, 3.32, 4.96, 6.50, 8.10 V by using LFE-5LMS and 1.13 V by using LFE-300CCM, respectively, and $J_L = -40$, -60, -80 mm/s, corresponding to voltages of 0.52, 2.72, 4.93 V, respectively. The flow conditions are investigated at a sensor position $L/D = 22$. The transparent wire mesh sensor (WMS) used in this study is shown in Fig. 3.

In order to clarify the accuracy of WMT on the void fraction measurement in the counter-current bubbly flow, a high-speed CCD camera (HSC) was set at the transparent WMS to investigate bubbles passing the sensor. An image sequence is captured at the same time of WMT measurement within 1 s. The high-speed CCD camera with 1000 frames per second (HSC-Fast Cam-Net 500/1000/Max, equipped with a standard NIKON 100 mm) is utilized to evaluate the void fraction. The setup of WMS and the high-speed CCD are illustrated in Fig. 4.

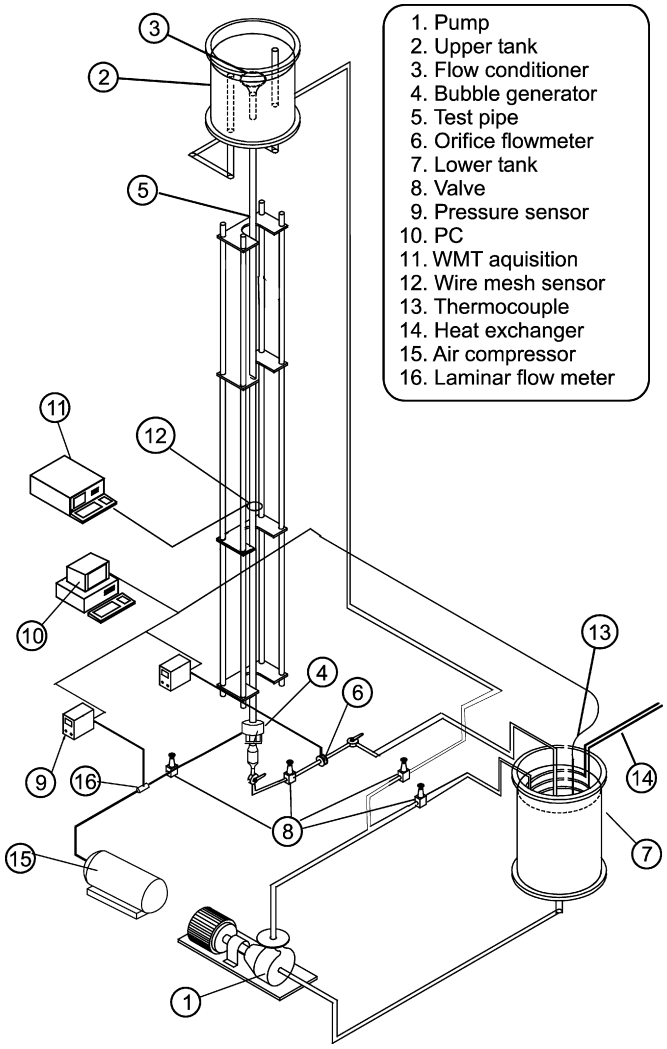

Fig. 1. Experimental apparatus.

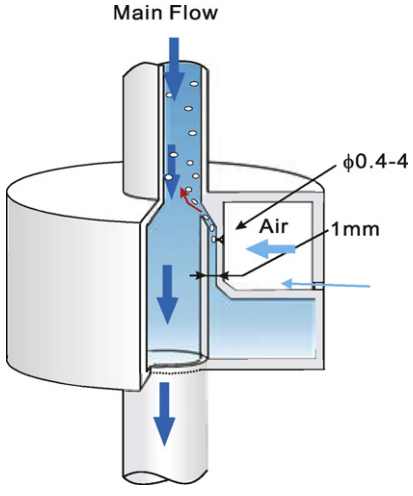

Fig. 2. Bubble generator.

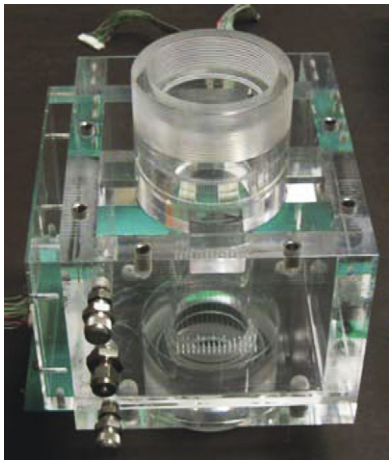

Fig. 3. Wire mesh sensor (WMS).

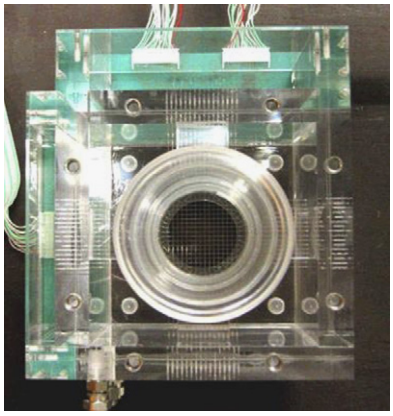

Fig. 5. Top view of WMS.

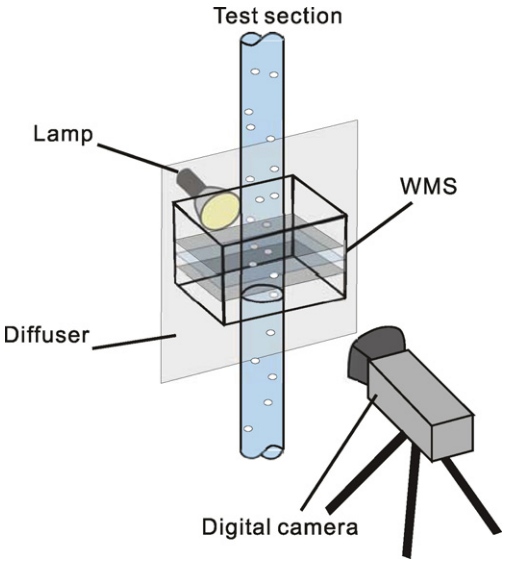

Fig. 4. The setup of optical method at a transparent WMS.

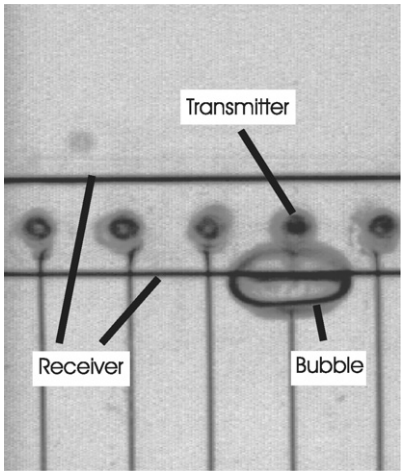

Fig. 6. Side view of WMS.

3. Wire mesh sensor

The transparent WMS used in this work was designed to cover an entire circular cross-section pipe with an inside diameter of 50 mm as shown in Fig. 5. Three layers of electrode wires in a square grid are placed through a pipe wall separated from each other by 2 mm. The middle plan is a transmitter plane while the upper and lower planes are receiver planes as shown in Fig. 6. Local instantaneous electrical conductivity is directly measured between all pairs of crossing wires. Each layer of wires consists of 16 × 16 wires corresponding to the spatial resolution of 2.94 mm × 2.94 mm with the wire diameter of 0.125 mm. The sensor delivers a sequence of two-dimension distributions of local instantaneous conductivity, measured in each mesh which is formed by two crossing wires. Local instantaneous void fractions are calculated assuming a linear dependence between void fraction and conductivity. So, the measured conductivity values are related to calibrated values obtained for the plain liquid in the measuring plane. The result is a three-dimensional data array $\varepsilon(x, y, t)$ where t are numbers of the instantaneous void fraction

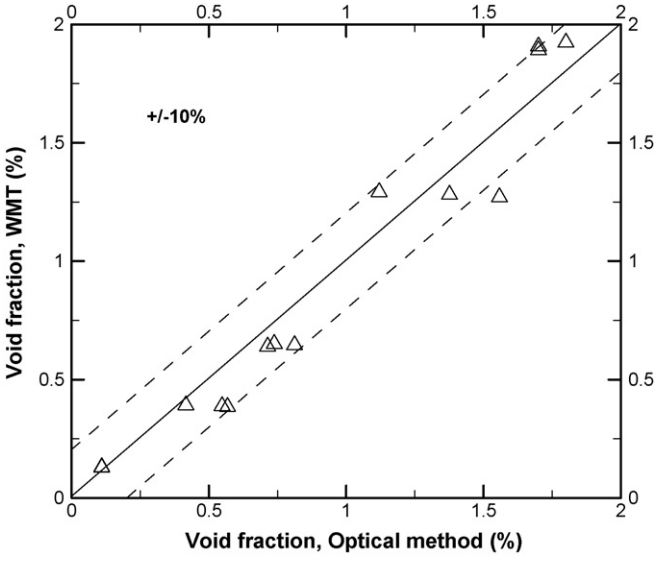

Fig. 7. Comparison of void fraction measurement between WMT and optical method.

distribution in time sequence and x, y are local measurement positions in a cross-section. A local time-dependent void fraction can be obtained directly from a linear relationship with the measured electrical conductivity as followed Eq. (1):

$$\varepsilon(x, y, t) = \frac{V(x, y, t) - V(x, y)^{W}}{V(x, y)^{A} - V(x, y)^{W}} \quad (1)$$

where $V(x, y)^{A}$ and $V(x, y)^{W}$ are voltages corresponding to plain air ($\varepsilon = 100\%$) and plain water ($\varepsilon = 0\%$), respectively. Cross-sectional time-averaged void fraction can be averaged directly from local time-dependent void fractions in 10 s.

4. Result and discussion

4.1. Accuracy of WMT on void fraction measurement in counter-current bubbly flow

There are many studies related to the accuracy of WMT on void fraction measurement. Cross-sectional void fraction measured by WMT was compared with the one measured by the optical method in a low void fraction range [9]. Furthermore, both local void fraction and cross-sectional void fraction measured by WMT were also compared with the one measured by X-ray method in a wide rage of void fraction [10]. However, the flow conditions in these studies were co-current and stagnant flow.

In order to use WMT for investigating counter-current bubbly flow, the accuracy of WMT on void fraction measurement for counter-current bubbly flow should be clarified. In this study, a non-intrusive optical method is carried out to measure the bubbly flow at the same condition with WMT. Detail of the camera setup is explained in the experimental setup section. For data processing of the optical method, bubbles images are taken with movie format within 1 s and converted sequentially to 1000 images. Twenty pictures are chosen consistently for calculation in each second. The commercial software, Image Pro, is used for obtaining bubble image information based on elliptic shape assumption. The difference between the cross-sectional

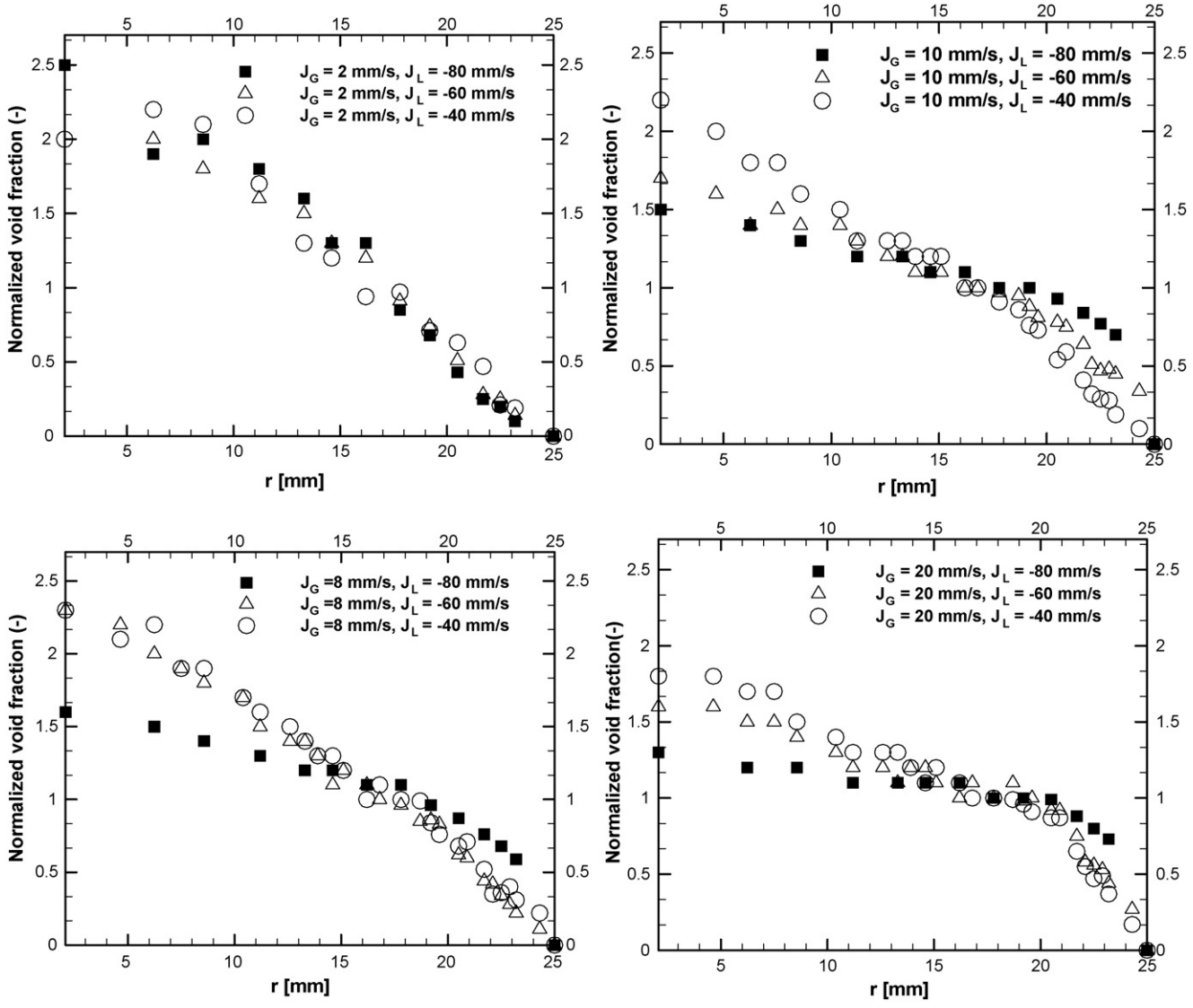

Fig. 8. Normalized void fraction depending on flow condition.

void fraction measured by WMT and the one measured by the optical method is within ±10% as shown in Fig. 7. Therefore, it is shown that the accuracy of WMT in counter-current bubbly flow is in the same order of magnitude with the one in stagnant and co-current bubbly flow [9,10]. It can be concluded that WMT can be used for investigating counter-current bubbly flow in the same way as the use in co-current and stagnant flow. However, there is a limitation of a non-invasive optical method at a high void fraction range because of the overlap of bubbles. Therefore, the accuracy of WMT in low void fraction range is only reported in this work.

4.2. Local void fraction characteristics of counter-current bubbly flow

An advantage of WMT is a capability of local parameters measurement. In this study, time-dependent local void fraction is obtained by WMT in 10 s. In this section, time-averaged local void fraction is shown and discussed. Normalized local void fraction profiles of the three superficial liquid velocity conditions with the same superficial gas velocity condition are displayed in Fig. 8. The normalized local void fraction is performed for investigating void profile characteristic affected by the superficial liquid and gas velocity. As we know that the local void fraction profile in the bubbly flow can be divided into five profiles including of wall-peak, intermediate peak, transition, flat and core-peak profile [12]. For a J_G of 2 mm/s, the core-peak profiles are observed at all superficial liquid velocity conditions. For a J_G of 8 mm/s, a local void fraction profile of a J_L of −80 mm/s is changed from the core-peak profile to the transition profile while the ones of the J_L of −60 and −40 mm/s are still the core-peak profiles. For a J_G of 10 mm/s, the local void fraction profile of the J_L of −80 mm/s is still the transition profile and the one of the J_L of −40 mm/s is still the core-peak profile. The local void fraction profile of the J_L of −60 mm/s is changed from the core-peak profile to the transition profile. For a J_G of 20 mm/s, the local void fraction profile of the J_L of −80 mm/s is changed from the transition profile to the flat profile and the one

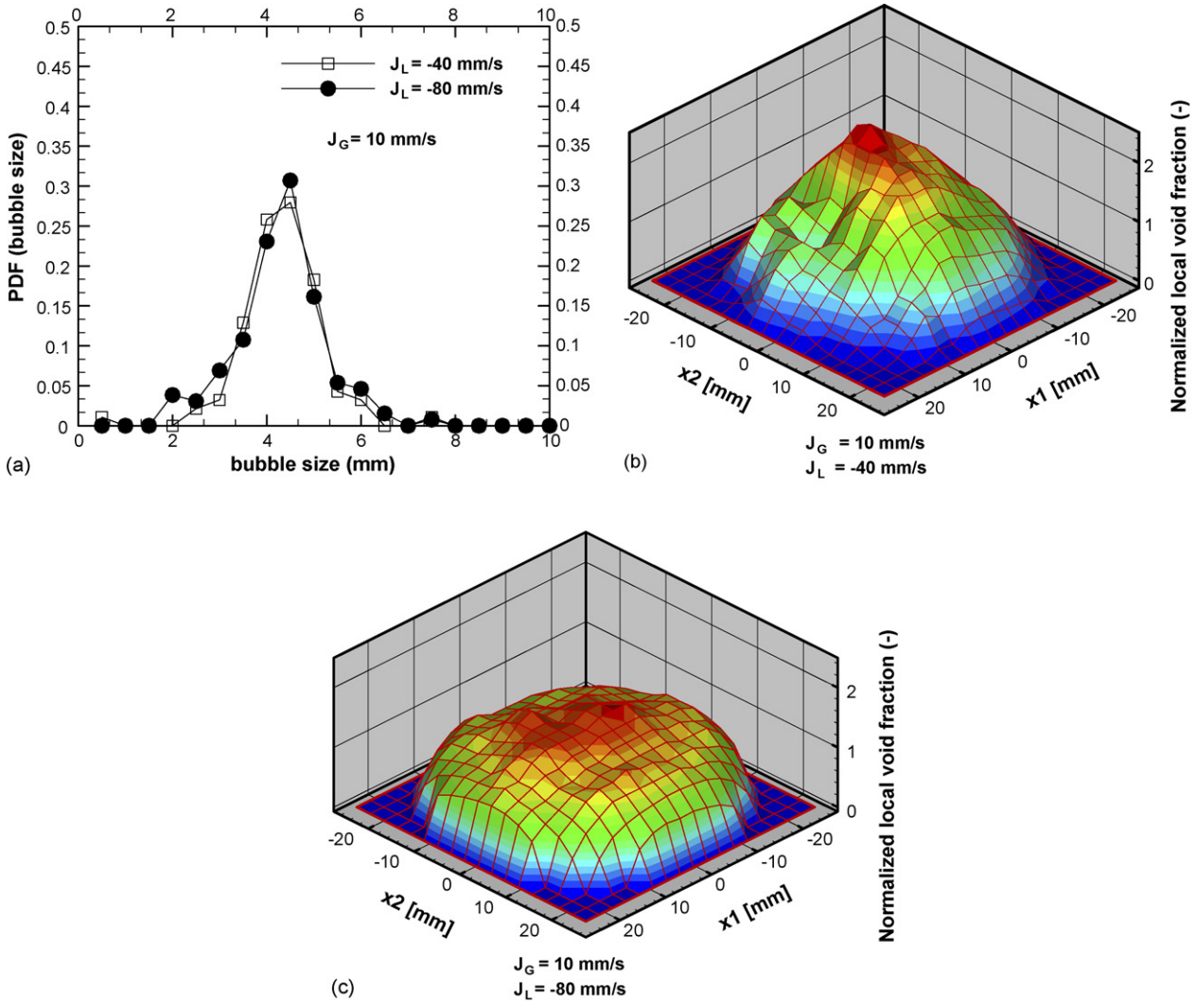

Fig. 9. (a) Bubble distribution of J_L of −40 and −80 mm/s at same J_G of 10 mm/s; (b) local void fraction of J_L of −40 mm/s and J_G of 10 mm/s; (c) local void fraction of J_L of −80 mm/s and J_G of 10 mm/s.

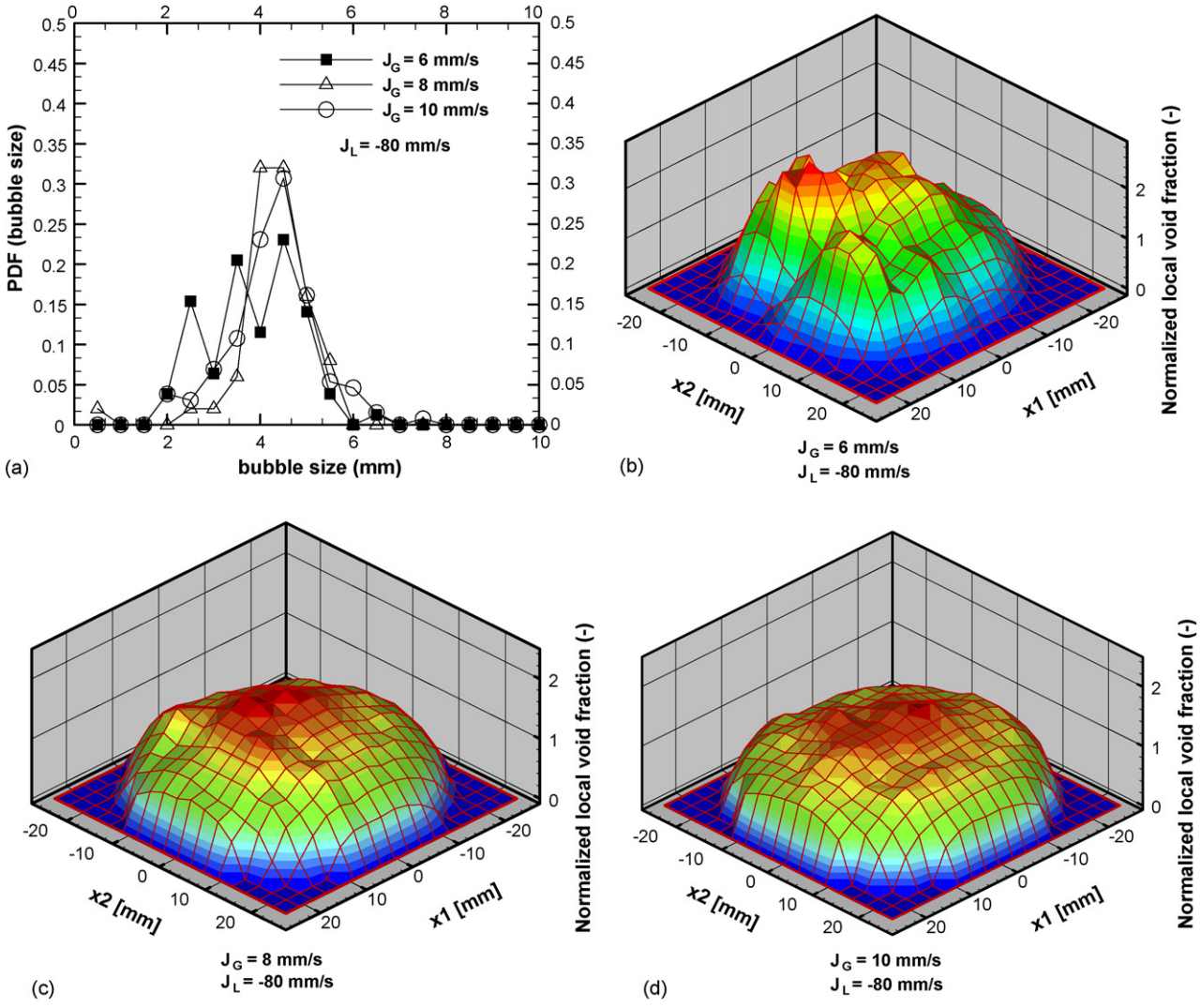

Fig. 10. (a) Bubble distribution of J_G of 6, 8, and 10 mm/s at same J_L of −80 mm/s; (b) local void fraction of J_G of 6 mm/s and J_L of −80 mm/s; (c) local void fraction of J_G of 8 mm/s and J_L of −80 mm/s; (d) local void fraction of J_G of 10 mm/s and J_L of −80 mm/s.

of the J_L of −40 mm/s is changed from the core-peak profile to the transition profile. The local void fraction profile of the J_L of −60 mm/s is still the transition void fraction profile. From Fig. 8, the local void fraction profiles are changed by superficial gas and liquid velocity conditions. The local void fraction profiles are changed from the core-peak profile to the transition and flat profile when the superficial gas and liquid velocity conditions are higher. These phenomena are affected by drag force attacking on bubbles because of the changing of bubble parameters and superficial liquid velocity.

The effects of superficial liquid velocity and bubble size on the local void fraction profile will be explained clearly. First, the effect of the superficial liquid velocity on the local void fraction profile will be discussed. The local void fractions of J_L of −40 and −80 mm/s at a J_G of 10 mm/s are shown in Fig. 9b and c. Bubble size information is obtained by a non-intrusive optical method. These two flow conditions have the same bubble distribution condition as also shown in Fig. 9a. The local void fraction profile of the J_L of −40 mm/s is the core-peak profile but the local void fraction profile of the J_L of −80 mm/s is the flat profile. The local void fraction profiles of these conditions are different because of the difference in liquid velocity. Second, the effect of bubble size on the void fraction profile will be discussed. The local void fractions of the J_G of 6, 8 and 10 mm/s at the same as the one of the J_L of −80 mm/s are shown in Fig. 10b–d, respectively. The bubble distribution obtained by a non-intrusive optical method of these three flow conditions are also shown in Fig. 10a. The bubble distributions of the J_G of 6 and of 8 mm/s are different, thus the local void fraction profiles of these conditions are also different. The local void fraction profile of the J_G of 6 mm/s is the core-peak profile while the local void fraction profile of the J_G of 8 mm/s is the flat profile. In another way, the bubble distributions of the J_G of 8 and 10 mm/s are quite the same, thus the local void fraction profiles of these conditions are the same. The local void fraction profiles of these conditions are flat profiles. From these comparisons, it can be concluded that the local void fraction profile is affected by the superficial liquid velocity and bubble distribution conditions.

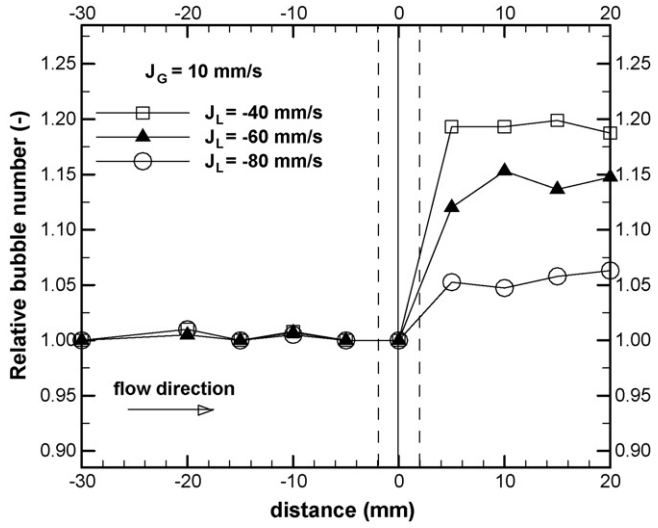

Fig. 11. Relative bubble number near a WMS.

4.3. Intrusive effect of WMS in counter-current bubbly flow

For the intrusive effect, there are two main intrusive effects of WMS on bubbles in the two-phase flow. The first one is the bubble break-up. The second one is the bubble deceleration. First, relative number of bubbles near a sensor obtained by a non-intrusive optical method is shown in Fig. 11. Bubbles passing WMS are broken by the sensor. The higher relative number of bubblers at downstream area comparing with upstream one can be seen. From three of J_L conditions, bubble velocity of a J_L of -40 mm/s is around 750 mm/s, bubble velocity of a J_L of -60 mm/s is around 600 mm/s, bubble velocity of a J_L of -80 mm/s is around 500 mm/s.

The bubble break-up rate increases following an increase in a bubble velocity. The lowest bubble break-up rate is at the value of the J_L of -80 mm/s. The highest bubble break-up rate is at the J_L of -40 mm/s condition. It can be concluded that the bubble break-up rate increase with increasing of bubble velocity. Second, bubble is decelerated by the sensor as shown in Fig. 12. The velocity of each bubble can be evaluated from the time that bubble migrated within the small axial length of 2 mm. The bubble velocity is estimated by averaging the leading and training bubble surface velocity. Bubbles passing WMT sensor are decelerated by the sensor. The bubble velocity is decreased about 40–50% of the upstream velocity. However, the velocity returns to an origin velocity after passing the sensor at 8 mm, four times of the wire layer distance in the sensor. From this figure, the bubble deceleration is not depending on J_L or the bubble velocity. Relative bubble velocities of the three J_L conditions are at the same dropping rate. These phenomena in counter-current bubbly flow are the same as the one in co-current bubbly [9]. It can be concluded that the bubble deceleration affected by WMS is not depending on the bubble velocity.

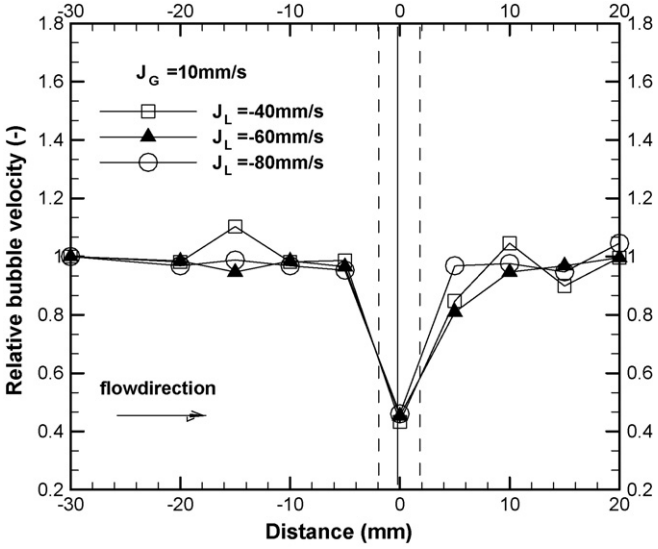

Fig. 12. Relative bubble velocity near a WMS.

5. Conclusion

In this work, wire mesh tomography (WMT) is applied for investigating characteristics of local void fraction in counter-current bubbly flow. The accuracy of WMT by comparing the result with a non-intrusive optical method is also clarified. The accuracy is within $\pm 10\%$. The accuracy of WMT in counter-current bubbly flow is in the same order as the magnitude with the one in stagnant and co-current bubbly flow. However, there is the limitation of a non-invasive optical method at a high void fraction range because of the overlap of bubbles. Therefore, the accuracy of WMT in the low void fraction range is only reported in this work. It can be concluded that WMT can be used for investigating counter-current bubbly flow in the same way with the use in co-current and stagnant flow. The local void fraction profile in counter-current bubbly is changed following the change of liquid velocity and bubble size. Furthermore, the intrusive effects of a wire mesh sensor (WMS) on void fraction measurement in counter-current bubbly flow are investigated. For the intrusive effect, there are two main intrusive effects of WMS on bubbles in the two-phase flow. The first one is the bubble break-up. The second one is the bubble deceleration. Bubbles passing WMS are broken and decelerated by the sensor. It can be concluded that the bubble break-up rate increase with increasing of bubble velocity. However, the bubble deceleration is not depending on the bubble velocity.

References

[1] K. Yamaguchi, Y. Yasaburo, Characteristics of counter-current gas-liquid two-phase flow in vertical tube, J. Nucl. Sci. Technol. 19 (12) (1982) 985–996.

[2] A.R. Hasan, C.S. Kabir, S. Srinicvasan, Counter-current bubble and slug flow in vertical system, Chem. Eng. Sci. 49 (16) (1994) 2567–2574.

[3] M. Aritomi, S. Zhou, M. Nakajima, Y. Takeda, M. Mori, Y. Yoshioka, Measurement system of bubbly flow using ultrasonic velocity profile monitor and video data processing unit, J. Nucl. Sci. Technol. 33 (12) (1996) 915–923.

[4] M. Aritomi, S. Zhou, M. Nakajima, Y. Takeda, M. Mori, Measurement system of bubbly flow using ultrasonic velocity profile monitor and video data processing unit(II) flow characteristic of bubbly countercurrent flow, J. Nucl. Sci. Technol. 34 (8) (1997) 783–791.

[5] M. Aritomi, S. Zhou, M. Nakajima, Y. Takeda, M. Mori, Measurement system of bubbly flow using ultrasonic velocity profile monitor and video data processing unit(III) comparison of flow characteristics between bubbly cocurrent and countercurrent flows, J. Nucl. Sci. Technol. 35 (5) (1998) 335–343.

[6] S. Richter, M. Aritomi, H.-M. Prasser, R. Hampel, Approach towards spatial phase reconstruction in transient bubbly flow using wire mesh sensor, Int. J. Heat Mass Transfer 45 (5) (2002) 1063–1075.

[7] H.-M. Prasser, D. Scholz, C. Zippe, Bubble size measurement using wire-mesh sensors, Flow Meas. Instrum. 12 (4) (2001) 299–312.

[8] H.-M. Prasser, E. Krepper, D. Lucas, Evolution of the two-phase flow in a vertical tube-decomposition of gas to bubble size classes using wire-mesh sensor, Int. J. Therm. Sci. 41 (2002) 17–28.

[9] W. Wangjiraniran, Y. Motegi, S. Richter, H. Kikura, M. Aritomi, K. Yamamoto, Intrusive effect of wire mesh tomography on gas-liquid flow measurement, J. Nucl. Sci. Technol. 40 (11) (2003) 932–940.

[10] H.-M. Prasser, M. Misawa, I. Tiseanu, Comparison between wire-mesh sensor and ultra-fast X-ray tomography for air–water flow in a vertical pipe, Flow Meas. Instrum. 16 (2–3) (2005) 73–83.

[11] H. Murakawa, H. Kikura, M. Aritomi, Mori, Measurement of bubbly flow in a vertical pipe using ultrasonic Doppler method, in: Proceedings of the FEDSM'03, Fourth ASME_JSME Joint Fluids Engineering Conference, Honolulu, Hawaii, USA, July 6–11, 2003.

[12] T. Hibiki, M. Ishii, Z. Xiao, Axial interfacial area transport of vertical bubbly two-phase flows, Int. J. Heat Mass Transfer 44 (10) (2001) 1869–1888.